Mol Divers (2014) 18:119–131
DOI 10.1007/s11030-013-9464-8

FULL-LENGTH PAPER

New insights in the activation of human cholesterol esterase to design potent anti-cholesterol drugs

Shalini John · Sundarapandian Thangapandian · Prettina Lazar · Minky Son · Chanin Park · Keun Woo Lee

Received: 10 April 2013 / Accepted: 19 July 2013 / Published online: 31 October 2013

Abstract Primary hypercholesterolemia is the root cause for major health issues like coronary heart disease and atherosclerosis. Regulating plasma cholesterol level, which is the product of biosynthesis as well as dietary intake, has become one of the major therapeutic strategies to effectively control these diseases. Human cholesterol esterase (hCEase) is an interesting target involved in the regulation of plasma cholesterol level and thus inhibition of this enzyme is highly effective in the treatment of hypercholesterolemia. This study was designed to understand the activation mechanism that enables the enzyme to accommodate long chain fatty acids and to identify the structural elements for the successful catalysis. Primarily the activation efficiencies of three different bile salts were studied and compared using molecular dynamics simulations. Based on the conformations of major surface loops, hydrogen bond interactions, and distance analyses, taurocholate was concluded as the preferred activator of the enzyme. Furthermore, the importance of two bile salt binding sites (proximal and remote) and the crucial role of 7 α-OH group of the bile salts in the activation of hCEase was examined and evidenced. The results of our study explain the structural insights of the activation mechanism and show the key features of the bile salts responsible for the enzyme activation which are very useful in hypolipidemic drug designing strategies.

Keywords Human pancreatic cholesterol esterase · Activation efficiency · Bile salts · Molecular dynamics simulation · Structural insights · Hypolipidemic agents.

Introduction

Human pancreatic cholesterol esterase (hCEase), which is also known as bile salt-activated or bile salt-dependent or bile salt-stimulated lipase, is secreted in pancreas and mammary glands. CEase is a serine hydrolase involved in the digestion of broad spectrum of substrates including triacylglycerides, cholesteryl esters, phospholipids, fatty acids, and esters of lipid-soluble vitamins. From its name we can understand that the activation of CEase depends largely on the presence of bile salts. The CEase remains inactive during its travel from pancreas to the small intestine. The CEase and chaperone Grp94 complex protects the enzyme from the proteolytic enzymes present in the duodenal environment during its travel. Upon the dissociation of the complex, CEase becomes active in the presence of bile salts [1–5]. The activity of CEase goes beyond just hydrolyzing the dietary lipids [6,7]. Plenty of evidence indicates that CEase may have deleterious effects in atherosclerosis because of the conversion of larger and anti-atherogenic high density lipoprotein to the smaller and atherogenic low density lipoprotein subspecies [8–11]. The function of plasmatic CEase in atherogenesis and its relationship with various pathological conditions are not clearly established [12]. Recently, inhibition of CEase has emerged as a potential therapeutic strategy especially in the development of hypocholesterolemic agents because

Electronic supplementary material The online version of this article (doi:10.1007/s11030-013-9464-8) contains supplementary material, which is available to authorized users.

S. John · S. Thangapandian · P. Lazar · M. Son · C. Park · K. W. Lee (✉)
Division of Applied Life Science (BK21 Program), Systems and Synthetic Agrobiotech Center (SSAC), Plant Molecular Biology and Biotechnology Research Center (PMBBRC), Research Institute of Natural Science (RINS), Gyeongsang National University (GNU), 501 Jinju-daero, Gazwa-dong, Jinju660-701, Republic of Korea
e-mail: kwlee@gnu.ac.kr

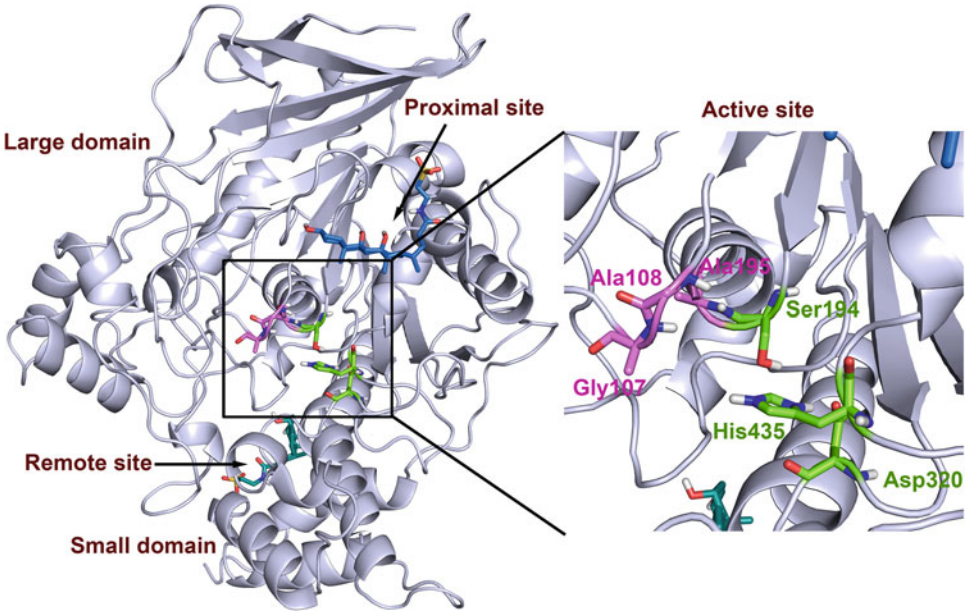

Fig. 1 Schematic representation of hCEase with its bile salt (TCH). The enlarged view of the active site displays catalytic triad and oxyanion hole amino acids represented in *green* and *pink color*, respectively. (Color figure online)

of its involvement in the control of plasma cholesterol level [13–17].

The CEase belongs to the α/β-hydrolase fold family and the members of this family share secondary and tertiary structural characteristics [18–20] and utilize the catalytic triad (Ser194, Asp320, and His435) residues for its mechanism. The catalytic domain of CEase contains large and small domains and the active site of this enzyme is present almost at the center of these two domains. The active site is majorly composed of the residues from the large domain (Fig. 1). The catalytic triad serves as general acid–base and nucelophilic catalytic entity together with an "oxyanion hole" composed of Gly107, Ala108, and Ala195 residues [1,21,22]. Bile salts have several effects on CEase as cofactors [23] and they bind at two different binding sites, proximal and remote, present in CEase. The proximal site is located close to the active site in the large domain and the remote site is located away from the active site in the region between large and small domains. The dependency of CEase on bile salts and its ability to hydrolyze long and short chain substrates makes it different from other lipases [24]. In humans, approximately 80 % of bile salts are the salts of taurocholic acid and glycocholic acid [25]. The study on carbamate-based inhibitors proved that bile salts enhance the hydrophobicity of both the cholesterol and fatty acid binding sites of CEase [10]. The efficiency of bile salts in the activation of the enzyme is unclear. Three different bile salts, taurocholate (TCH), cholate (CHA), and glycocholate (GCH), were used in this study and the main difference between these three bile salts is their chemical side chains. Binding of two bile salts (proximal and remote) are important, but the contribution of proximal bile salt is higher than the remote bile salt in terms of the activation of CEase. There are three major lipases secreted by pancreas and only CEase requires bile salts for its activation. Especially the presence of bile salt containing 7 α-OH group and its specific interaction are necessary for the hydrolysis of water-insoluble lipid esters [4,26].

A comprehensive molecular level understanding of the activation of this enzyme by bile salts is inevitably necessary to design potent inhibitors in the treatment of cardiovascular diseases. In order to obtain that, a detailed study was performed with the following objectives: (i) to compare the activation efficiency of three different bile salts such as TCH, CHA, and GCH via observing structural changes induced by them, (ii) to study the importance of both the proximal and remote bile salts and their involvement in the activation of the enzyme, and (iii) to observe the importance of the presence of 7 α-OH group in TCH and its key interactions that are involved in the activation of the enzyme.

Materials and methods

Preparation of systems

The solved crystal structures of hCEase and bovine CEase (bCEase) were obtained from the Protein Data Bank (PDB) and used in the molecular dynamics (MD) simulations. A total of 7 systems, including an apoform and 6 complexes with different and modified bile salts, were prepared and used in this study (Table 1). The three different bile salts, utilized were TCH, CHA, and GCH. The systems were named based on the name of the ligand present in the hCEase complex. Thus, the names hCEase_TCH, hCEase_CHA, and hCEase_GCH represent the three different bile salt bound complexes of hCEase. As mentioned earlier, two bile salt binding sites are present in hCEase. In the second study in order to avoid confusion, the systems were named according

Table 1 Systems and their details used in MD simulations

System no.	System name	Name of ligands	No. of ligands	Water molecules	Counter ions (Cl^-)
1	hCEase_Apo	–	–	27,751	6
2	hCEase_TCH	TCH	2	27,708	6
3	hCEase_CHA	CHA	2	27,722	6
4	hCEase_GCH	GCH	2	27,709	6
5	hCEase_Prx	TCH-prx	1	27,728	5
6	hCEase_Rmt	TCH-rmt	1	27,748	5
7	hCEase_XOH	TCH_XOH	2	27,710	4

to their number and position of ligands. The system without bile salt (non-ligated system) was named hCEase_Apo, the system with the bile salt (TCH here) present at both proximal and remote region (double-ligated system) was named hCEase_TCH. The systems with only one bile salt (single-ligated systems) were named hCEase_Prx and hCEase_Rmt in which TCH is present at the proximal and remote sites, respectively (Fig. S1). In the third study, a modified TCH with no 7 α-OH group was used as a ligand and this system was named as hCEase_XOH. The initial coordinates of the enzyme and bile salts were obtained from the X-ray crystal structures of hCEase (PDB code: 1F6W) and bCEase (PDB code: 1AQL), respectively. The insignificant water molecules and ions were removed from these crystal structures.

Molecular dynamics (MD) simulations

The MD simulations of all 7 systems were performed under the same conditions using the GROMACS 4.5.3 package with the GROMOS96 force field [27,28]. The particle mesh Ewald (PME) method was used to treat long-range electrostatic interactions. The topologies of the ligand molecules were generated using the PRODRG web server [29]. The PRODRG server generates topology information for small molecules that are attuned with the GROMOS force field. The process of topology generation, output structure, and parameters were monitored with extra care. The apo and complex forms of the protein were immersed separately in a cubic box containing pre-equilibrated single point charge (SPC) water models. The dimensions of the cubic boxes are constructed in such a way that the box is extended approximately 1 nm from the edge of the protein molecule in all dimensions. As a result of the box size nearly 30,000 water molecules were added for each system. In order to neutralize the overall net charge of the systems number of Cl^- counter ions were added to individual systems by replacing the water molecules. The systems were energy minimized, so as to remove the internal restraints due to the crystal packing, for 10,000 steps using steepest descent algorithm.

Following energy minimization, a 100 ps position restrained MD run was carried out with the backbone of the protein immobilized to allow the added water molecules equilibrate around the protein. Then, the production run was performed for 5 ns in the isothermal–isobaric (NPT) ensemble. The temperature and constant pressure were maintained with a reference value of 300 K and 1 atm, respectively [30]. A twin-range cutoff was used for long-range interactions including 0.9 nm for van der Waals and 1.4 nm for electrostatic interactions. The MD simulation calculations were performed using the periodic boundary conditions (PBC) to eradicate the boundary effect. All the bonds comprising hydrogen atoms were constrained using the LINCS algorithm whereas the geometry of the water molecules was constrained using the SETTLE algorithm. The time step was fixed to 2 fs to integrate the equations of motion. During the production run, the coordinates of the individual systems were saved for every 1 ps. The data analysis was carried out using essential dynamics (ED) method to divide out the combined inner gestures in the protein structures. The basic calculations such as atomic root mean square deviation (RMSD), Cα–root mean square fluctuation (RMSF), various energies, and radius of gyration (Rg) were carried out using the MD simulation analysis package available in GROMACS.

Essential dynamics (ED) analysis

The ED analysis is considered a potent tool to distinguish the inappropriate local fluctuations in a protein from its configuration space [31]. The ED methodology, which is similar to the multidimensional linear square fit, was applied to the protein dynamics by Garcia for the first time [32]. This essential degree of freedom can be used to define the overall and the interrelated motions that are relevant to the biological function of several proteins [33–43]. The ED analysis was performed using two subroutines g_covar and g_anaeig available in GROMACS. The ED analysis was carried out by first fitting the protein coordinates recorded in the trajectory to the initial structure to remove all the rotational and translational motions followed by the building of covariance

matrices of atomic positional deviation [44]. The constructed covariance matrices were then diagonalized to create a new matrix whose elements are eigenvectors and corresponding eigenvalues that indicate the component and amplitude of atomic fluctuations, respectively [45]. The extreme structure was obtained by the projection of recorded trajectories on the largest eigenvectors. The extreme structure gives spontaneous ideas about the specific direction of motion.

Results and discussion

Comparison of activation efficiency of different bile salts

In this part of the study, three different bile salts namely TCH, CHA, and GHA complexed with hCEase were used for the comparison of their activation efficiency. First, to check the conformational variations and the overall stability of the three MD simulations systems, the basic physical properties including the backbone RMSD, Cα–RMSF, potential energy, and Rg were calculated and discussed (Text S1-1.1, 1.2; Fig. S2).

Hydrogen bond network

The intermolecular hydrogen bonds (H-bonds) between the protein and different ligand molecules were calculated and compared. In the proximal site, TCH has shown stable and strong H-bonds, a maximum of 6 and an average of 3.3, when compared to GCH and CHA. GCH has shown considerable number of H-bonds, a maximum of 7 and an average of 2.4 whereas CHA has formed a maximum of 3 and an average of 0.3 H-bonds during the simulation (Fig. 2a). In the remote site, TCH has shown strong H-bond interactions, a maximum of 11 and an average of 7, throughout the simulation. The CHA, which has shown unstable and minimum interaction in the proximal site, has shown a maximum of 5 and an average of 2.6 H-bonds. Interestingly, GCH that formed stable and considerable interactions in the proximal site has shown unstable interactions with a maximum of 1 and an average of 0.03 that is nearly no H-bonds (Fig. 2b). From this analysis, we observed that TCH has formed very stable and strong H-bond interactions at both the sites compared to CHA and GCH that formed strong interactions at either proximal or remote site. Hence, it is clear that the TCH is capable of maintaining stable and strong H-bond interactions at both the sites of hCEase. The important residues having interactions with different bile salts were identified using Discovery Studio (DS) 2.5, Ligplot [46], and Poseview [47] programs.

Structural changes and binding mode analyses

In order to check the efficiency of three different bile salts, the binding mode and conformational changes of surface loops present around the active site were investigated. As mentioned earlier, the conformational changes of surface loops were considered important for the activation of hCEase. The representative structures obtained from MD simulations were selected for structural analysis. The surface loop movements observed in TCH were compared with CHA and GCH systems to investigate the key difference and as a result the loop movement of TCH is greater than CHA

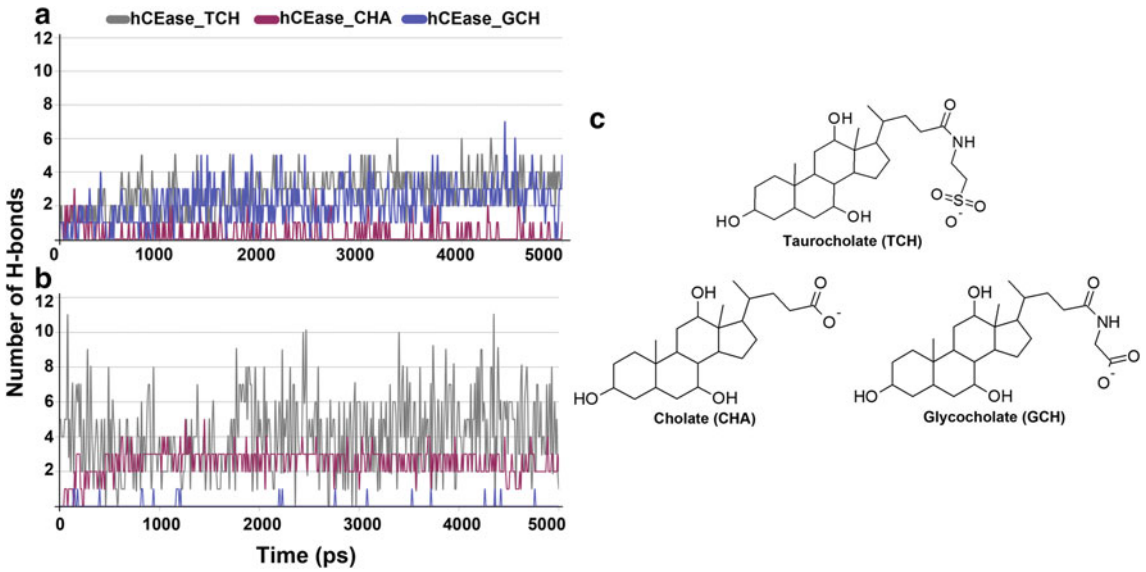

Fig. 2 H-bond plot and 2D structures of TCH, CHA, and GCH. The number of H-bonds interactions between protein and ligand molecules, at the **a** proximal and **b** remote sites, throughout the MD simulations. It was evident through the comparison of H-bond interactions formed by the ligands that TCH binds both the active sites tightly compared to other ligands. **c** The 2D structures of three different bile salts

and GCH (Fig. S3). The binding modes of three bile salts, at their corresponding site of the enzyme, were also compared to explain the differences in their surface loop movements. Initially, 2D chemical structures of the three bile salts were compared and these bile salts differ only at their side chains (Fig. 2c). The TCH, CHA, and GCH contain the side chains of –(acetylamino)ethanesulfonate, –acetate, and –(acetylamino)acetate groups.

The binding mode of TCH (Fig. 3a) was observed in such a way that its side chain was snuggly binds in between 120 and 450 loops thereby it has strong interactions (Fig. 3b) with both the loop residues. The strong interactions and stable binding mode of TCH did not disturb the catalytic site residues and the size of the catalytic site. Such strong interactions with the loop residues were missing in case of CHA and GCH. The binding mode of CHA (Fig. 3c) was not stable due to the weak interactions with the loop residues (Fig. 3d) thereby it disturbed the catalytic site residues. The binding mode of GCH is also very much different than that of TCH (Fig. 3e). The GCH has shown strong interactions with the 450-loop residues compared to the 120-loop residues (Fig. 3f) and due to the unfavorable binding mode the catalytic site residues were disturbed. The key reason for the differences in their binding modes was brought through the differences (Fig. 2c) in their side chains (Text S1-1.3).

Distance analyses

The active site of CEase consists of catalytic triad and "oxyanion hole" residues that are conserved in all known lipases. The spatial arrangement and sequential order of these three residues are the most conserved structural features in the α/β hydrolase fold family. The catalytic triad residues Ser194, Asp320, and His435 serve, respectively, as nucleophile and proton shuttle to form the charge-relay network. The conserved residues other than catalytic triad in all the known members of CEase family are buried partially around His435. These residues are Glu193, Asp434, Asp437, and Asp438 [5]. The main role of these residues is to assist His435 in transporting protons. During the catalytic process, a putative "oxyanion hole" was formed by the backbone amide groups of the residues Gly107, Ala108, and Ala195 to stabilize the tetrahedral transition state of the substrate. Hence,

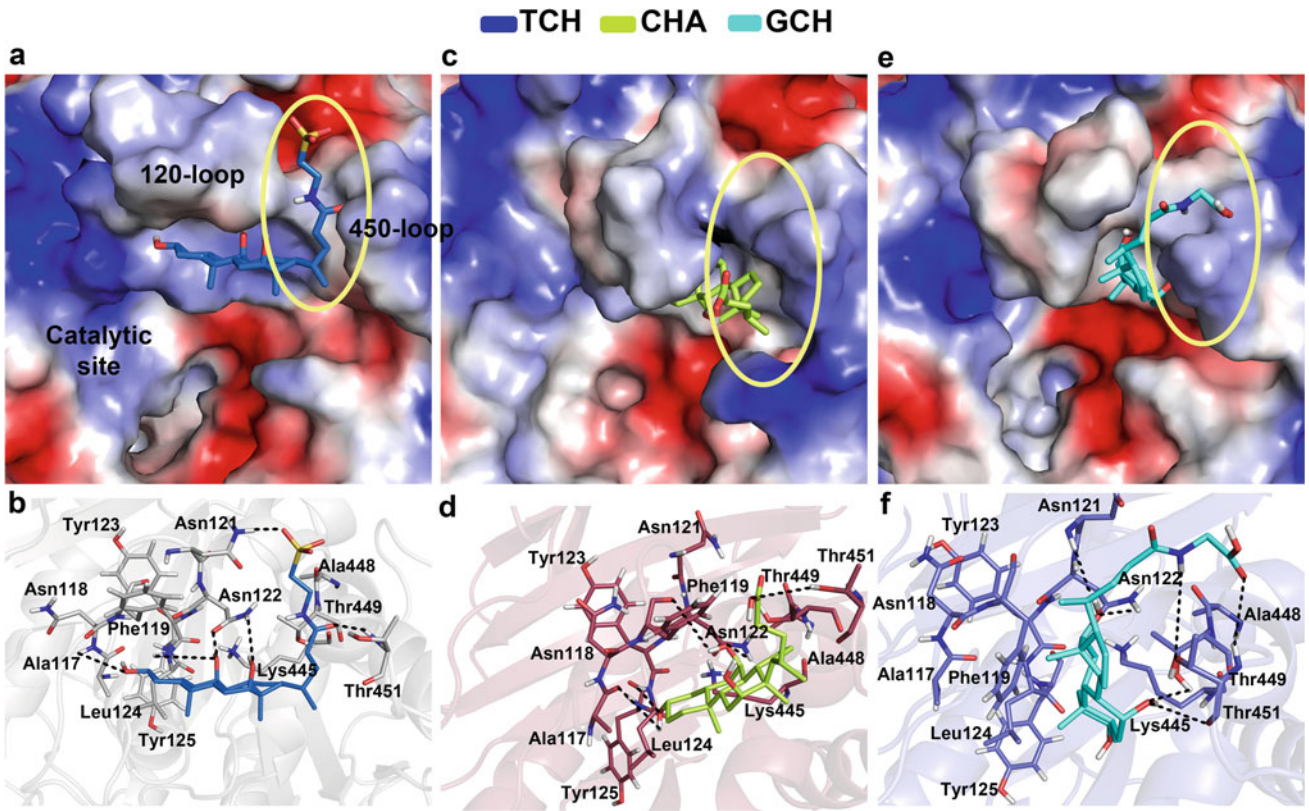

Fig. 3 Binding modes of three different bile salts. The binding mode of **a** TCH, **c** CHA, and **e** GCH, at the proximal site of the hCEase showing their influence on the catalytic site and the H-bond interactions between protein and **b** TCH, **d** CHA, and **f** GCH. The binding mode of TCH was observed to be stable and brought the necessary changes to catalyze the long chain fatty acids. The *gray*, *raspberry*, and *violet colors* represent hCEase with TCH, CHA, and GCH, respectively. The H-bond interactions are shown in *black dashed lines*. (Color figure online)

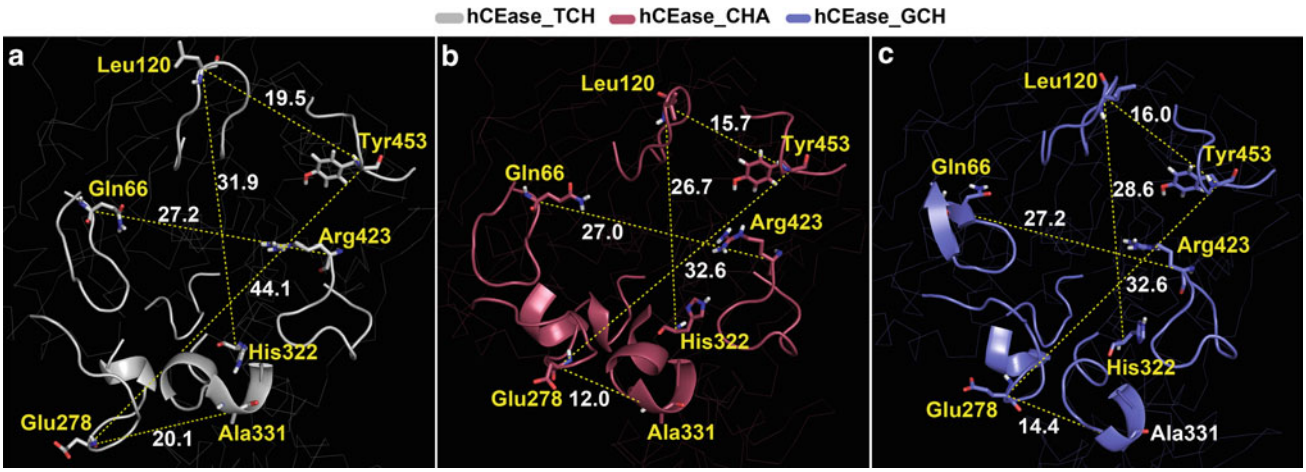

Fig. 4 Distances between key residues of the surface loops. The distance between the key residues in the surface loops of **a** hCEase_TCH, **b** hCEase_CHA, and **c** hCEase_GCH. The key residues are shown in *stick form* and the important loop regions are shown in *cartoon form*. The distances are shown in *yellow dotted lines* in Armstrongs. (Color figure online)

the distance between these residues is very crucial to trigger the catalytic mechanism (Text S1-1.4).

The size of the active site was evaluated by measuring the distance between the key residues in the surface loops (Fig. 4). The distances between the key residues, Glu278 & Tyr453, Leu120 & His322, Glu278 & Ala331, Gln66 & Arg423, and Leu120 & Tyr453, in the surface loop regions were measured. The hCEase_TCH has shown maximum distance values between four main residue pairs, Glu278 & Tyr453, Leu120 & His322, Glu278 & Ala331, and Leu120 &Tyr453 with the values of 44.1, 31.9, 20.1, and 19.5 Å, respectively. In case of hCEase_CHA, the four main residue pairs have shown less distance values of 32.6, 26.7, 12.0, and 15.7 Å. Similarly, in hCEase_GCH the distance between four key residue pairs was 32.6, 28.6, 14.4, and 16.0 Å which is far less than that of hCEase_TCH. The other pair, Gln66 & Arg423, has shown similar distance in all the three systems with the considerable values of 27.2, 27.0, and 27.2 Å, respectively. The maximum distances in hCEase_TCH indicate that the surface loops moved away to bring forth the open conformation thereby the size of the active site is bigger than hCEase_CHA and hCEase_GCH systems. In order to confirm this result, the distances between the key residues in the surface loops of hCEase_TCH, hCEase_CHA, and hCEase_GCH were measured throughout the simulation time. From the calculations, the maximum distances between the key residues Glu278 & Tyr453, Leu120 & His322, Glu278 & Ala331, Gln66 & Arg423, Leu120 & Tyr453, and Leu120 & Thr451 (4.0, 3.1, 1.8, 2.3, 1.6, and 1.5 nm, respectively) were observed in hCEase_TCH. But these distances were comparatively less in hCEase_CHA and hCEase_GCH systems except the distance between Gln66-Arg423 which is similar in all systems (Fig. 5). The distance analysis evidenced that the active site of hCEase_TCH favors the binding of long chain fatty acids than the other two systems. Hence, TCH may act as a preferable activator of hCEase when compared to CHA and GCH. The interaction energetics between protein and ligand are discussed in Text S1-1.5 of supporting information.

Importance of both bile-salt binding sites (proximal and remote)

Two bile-salt binding sites are present in hCEase namely proximal and remote sites and one of these sites is involved significantly in the activation of hCEase compared to another, though both are required. So the main aim of this study is to investigate the roles of both the bile salts in the activation of the enzyme. In this part of study, analyses of non-, single-, and double-ligated systems were considered to observe the importance of the presence of both bile salts. The overall structural stability of all the systems was investigated through the calculation of RMSD, RMSF, and energy terms throughout the simulation (Text S2-2.1; Fig. S5).

Intermolecular hydrogen bonds

The intermolecular hydrogen bonding between the protein and ligand plays an essential role in stabilizing the protein–ligand complexes. The stability of H-bond network formed between TCH (proximal and remote) and hCEase was calculated throughout the simulation for all the ligated systems (Fig. 6). The proximal bile salt binding region is located between 120 and 450 loops. The residues of these two loops are found to be very important for the proximal TCH binding. The residues around remote TCH molecule were con-

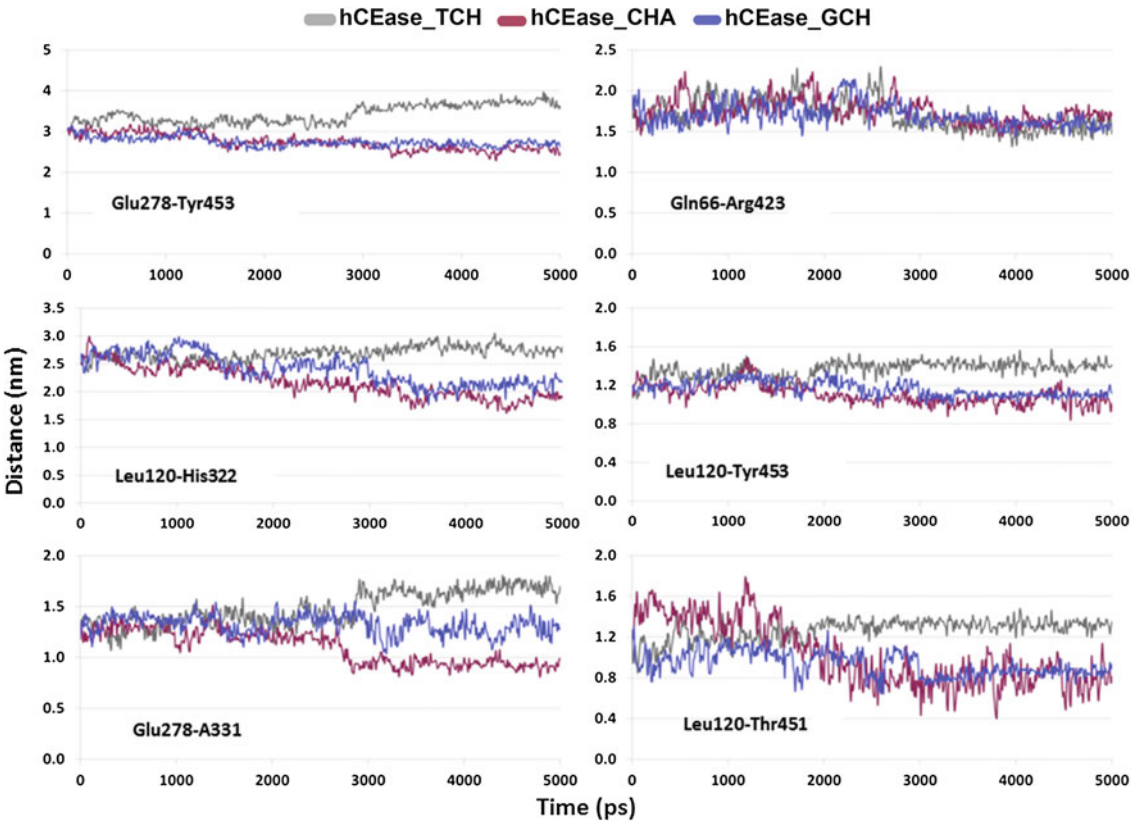

Fig. 5 Distances between key residues during MD simulations. The distance between the key residues of hCEase_TCH, hCEase_CHA, and hCEase_GCH was measured throughout the MD simulations. The distances are measured in nm scale. The TCH complex has shown greater distances compared to CHA and GCH

sidered important for its binding. In order to avoid confusion, the systems were named according to the position of the ligand in hCEase. The proximal and remote TCH present in double-ligated (hCEase_TCH) system were named TCH-prx and TCH-rmt, respectively, whereas the proximal and remote TCH present in single-ligated systems, hCEase_Prx and hCEase_Rmt, were named Prx-prx and Rmt-rmt, respectively.

First, the H-bond networks formed individually by proximal and remote TCH were compared. The TCH-prx has shown stable and maximum number of H-bond interactions (Fig. 6a) with an average value of 3.3 and a very stable binding mode as a result of the strong interaction with the loop residues (Fig. 6b). The H-bond interactions of Prx-prx were reduced to an average value of 1.3 throughout the simulation. The reason for the difference was observed from the comparison where the binding mode of Prx-prx was totally disturbed due to the lack of strong interaction with the loop residues (Fig. 6c). In the first 2 ns of MD simulation, both the systems have shown similar number of H-bonds but later the interaction between TCH-prx and protein has become stronger with the maximum of 6 and minimum of 3 H-bonds (Fig. 6a). The H-bond information of TCH-rmt is available in Text S2-2.2 and Fig. S6.

Structural analyses

The representative structures of the four systems (hCEase_Apo, hCEase_TCH, hCEase_Prx, and hCEase_Rmt) were picked from the last 3 ns of MD simulation for structural analysis. This analysis was carried out to understand how a bile salt influences the active site and the overall structure of hCEase. The conformational changes of the loops present around the active site play very important roles in the activation of hCEase. Hence, the conformational changes of these 6 surface loops present around the active site are mainly discussed in this part of the study. The loops were named according to their residue numbers.

Conformational changes of 120-loop

The 120-loop (residues 115–125) is located in the proximal binding site and it has been suggested that the conformational change of this 120-loop is involved in the activation

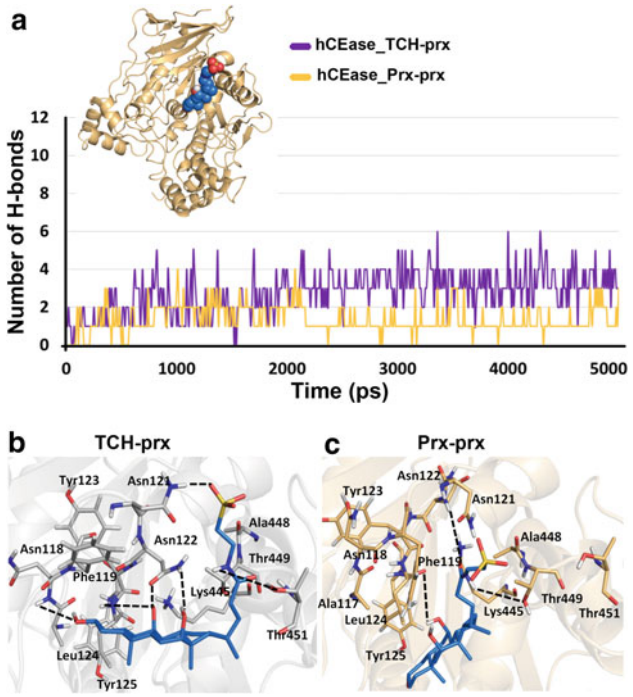

Fig. 6 H-bond interactions and binding mode of TCH at the proximal site. **a** The number of H-bond interactions between protein and proximal ligands of hCEase_TCH and hCEase_Prx were measured throughout the MD simulations. **b**, **c** Binding modes and H-bond interactions of TCH-prx and Prx-prx. The interacting residues at the proximal sites of hCEase_TCH and hCEase_Prx are shown in *white* and *yellow-orange color sticks* while the ligands are shown in *blue sticks*. The H-bond interactions are shown in *black dashed lines*. (Color figure online)

of hCEase. Many studies that were carried out on the primary sequence of lipase/esterase family have revealed that the 120-loop region of all known CEases is composed of the consensus sequence of GANFLXNYLYDGEE, where X is the variable. The 120-loop was found in a closed conformation in the apoform of the enzyme. It has been reported that the open conformation of the 120-loop is required for the activated hCEase [1,5]. Our MD simulation results have shown the expected 120-loop movement upon the binding of proximal TCH as observed in the activated structure of bCEase (Fig. S7). Therefore, this confirms the statement that the proximal bile salt influences the loop conformation and leads to the activation of hCEase. In the absence of proximal TCH, 120-loop is in the closed conformation and the 450-loop (residues 447–458) was present outside the bile salt binding cavity at the same time. Before the binding of TCH (apoform), all the loops were in the closed conformation and particularly the closed conformation of the 120-loop nearly blocked the part of the active site where the big steroid moiety of the substrate binds. The substrate-bound structure of *Candida cylindracea* CEase, which is a homologue to the hCEase, revealed that the position of the 120-loop and the cholesterol moiety of the substrate were present in an overlapping position and thus the loop has to move away for the substrate to bind comfortably [48]. The 120-loop moves away and brings the 450-loop inside when proximal TCH approaches and thereby making it suitable for its binding. In order to check the degree of movement of the 120-loop during MD simulation the distance between Leu120 residue in the ligated and non-ligated systems was measured. These distance values with respect to the apoform are 9.5, 9.2, and 4.4 Å in hCEase_TCH, hCEase_Prx, and hCEase_Rmt systems, respectively (Fig. S8). This comparison of 120-loop movement in different systems gives a clear idea that the eminent conformational changes were observed in the double-ligated system in which proximal TCH plays a crucial role. The changes in other loops and catalytic site are discussed in Text S2-2.3, 2.4.

Major binding sites of CEase substrate

There is no crystal structure available for hCEase–substrate complex in PDB. The active site of hCEase is similar to the active sites of *Pseudomonas cepacia* lipase and *Candida rugosa* lipase that contain substrate-bound crystal structures in PDB [49–51]. By comparing the crystal structures, it has been observed that the active site of hCEase will possibly have five major binding sites: (i) alkyl chain binding site—accommodates the alkyl and acyl chains of substrates like triacylglycerol and cholesteryl ester, respectively, (ii) esteratic site—consists of catalytic triad residues that are involved in the nucleophilic attack and general acid–base catalysis, (iii) second alkyl chain binding site—accommodates the alkyl chain that is attached with the five membered ring of the triacylglycerol and this is present in a cleft above the catalytic site, (iv) oxyanion hole—involved in the stabilization of transition state of the substrate during catalytic process, (v) leaving hydrophilic group binding site—located in the opposite direction of the alkyl chain binding site and binds to the hydrophilic part of the leaving group, and (vi) leaving hydrophobic group binding site—binds to the hydrophobic part of the leaving group [3].

The changes in the active site of hCEase were examined and it was compared with the proposed major binding sites reported for hCEase. The main purpose of this analysis is to monitor how the substrate binding sites influenced by the binding of TCH in the double-ligated system. The alkyl chain binding site is present in the 270-loop region whereas the second alkyl chain binding site and the leaving hydrophobic and hydrophilic group sites are close to the 120-loop. These two important loop regions have largely undergone favorable conformational changes for the binding of large substrate molecules. The esteratic site and "oxyanion hole" are in the catalytic site and this was stable and did affect the arrangements of the catalytic site residues and their

distances. Thereby it is suitable for the binding of long chain as well as small chain substrate molecules.

Essential dynamics (ED) analysis

The ED analysis or principal component analysis is a powerful tool, which is commonly utilized in MD simulation studies, to identify the functionally relevant large-scale cooperative motions. The ED analysis was carried out for four systems, namely, hCEase_Apo, hCEase_TCH, hCEase_Prx, and hCEase_Rmt. The results were used to envision the region with the predominant movements that can possibly be important for the biological function of the protein. The extreme structures were extracted to monitor the greatest movement from the principal component of each system. The Cα–Cα distance of the four systems was measured and the maximum deviations were observed in all the four systems (Fig. 7).

The hCEase_Apo did not show any significant movement whereas in hCEase_TCH the maximum movement was observed in the 270-loop region which is one of the important surface loops (Fig. 7a, b). Similarly upon proximal TCH binding the 270-loop movement was high (Fig. 7c). The hCEase_Rmt did not show any considerable movement in the 270-loop but instead showed a maximum movement in the 450-loop (Fig. 7d). Hence, both the TCH are needed but the contribution from proximal TCH is prominent. Interestingly, all the greatest movements observed in the ligated systems were from the surface loop regions especially the 270-loop which is considered very important for the binding of substrate. From this study, it is observed that maximum deviations obtained from ED analysis correlate well with the biological action. This result supported our studies that the movement of surface loop residues plays a very important role in the activation of CEase.

Importance of 7 α-hydroxyl group in TCH

CEase hydrolyzes triacylglycerols and cholesteryl esters more effectively with the bile salts containing 7 α-OH group and this signifies that such specific interactions are necessary for the activation of the enzyme. However, the structural explanation for this concept was not clear. Hence, this study was carried out to investigate the role of 7 α-OH of TCH in the activation of hCEase. To prove the importance of 7 α-OH group, a system of hCEase complexed with a modified TCH (hCEase_XOH) with no 7 α-OH group (TCH_XOH) was prepared and subjected to MD simulation and the results were compared with hCEase_TCH system. Basic analyses were performed to ensure the overall system stability and the results are discussed in supporting information along with the 2D chemical structures (Fig. S12) of TCH and TCH_XOH (Text S3-3.1; Figs. S13, S14).

Analysis of intermolecular hydrogen bonds

The number of H-bond interactions between the protein and the ligand in the proximal and remote regions were calculated. Remarkably, noticeable difference was observed between the two systems. In the proximal site, the binding of

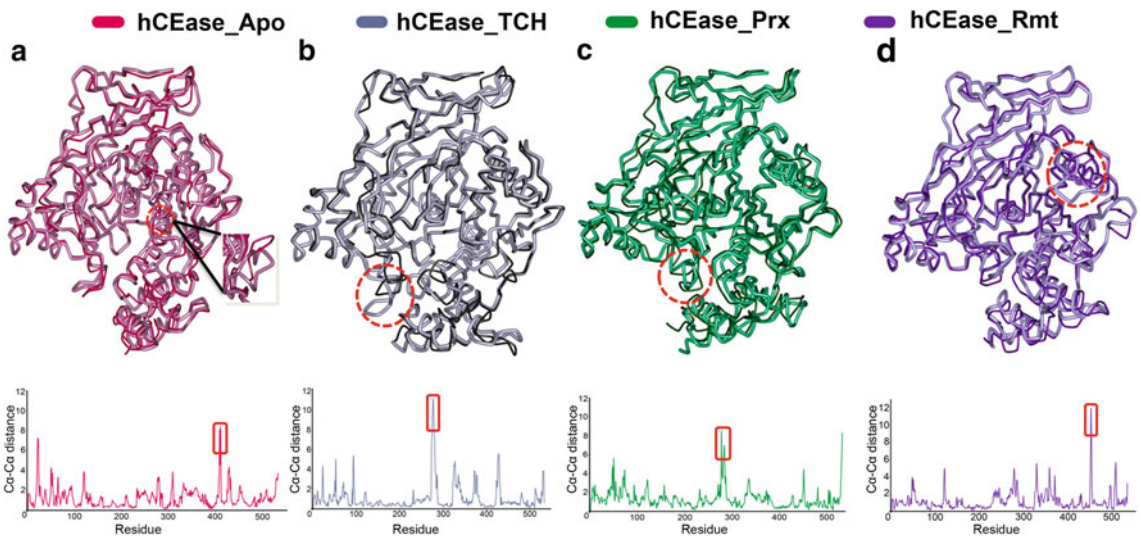

Fig. 7 The essential dynamics analyses of four systems. The maximum correlation motions were scrutinized for **a** hCEase_Apo, **b** hCEase_TCH, **c** hCEase_Prx, and **d** hCEase_Rmt systems. The maximum and minimum projections of the two protein trace structures along with the largest eigenvector were superimposed in order to show the maximum correlation motion of each residue. The maximum and minimum projection structures are given in *light* and *dark colors*. The Cα–Cα distance plots between superimposed structures are given for each system below its structures

TCH was stable without affecting the catalytic site (Fig. 8a) whereas the binding of TCH_XOH was not stable and affected the catalytic site (Fig. 8c). The reason for the differences in their binding mode was explained through H-bond analysis. The TCH-prx has established strong interaction with the loop residues Phe119 and Asn122 through the 7 α-OH group. This interaction also enables TCH to strongly interact with other key residues such as Ala117, Asn121, and Thr451 (Fig. 8b). But such interaction and assistance were missing in hCEase_XOH system due to the absence of 7 α-OH and TCH_XOH moved closer toward Arg63 and Tyr75 by forming strong H-bonds with them (Fig. 8d). The TCH-prx has formed stable and strong H-bonds, a maximum of 6 and an average of 3.3 but the H-bonds formed by TCH_XOH-prx were reduced to half, a maximum of 3 and an average of 1.6, throughout the simulation (Fig. S15a, b). The H-bond information of TCH-rmt and interaction energetics between protein and ligand are available in Text S3-3.2 and 3.3.

Structural changes

The structural analyses revealed that the binding of TCH_XOH was not appropriate to bring the open conformation of the 120-loop and other surface loops. The distance between the positions of Leu120 in hCEase_TCH and hCEase_XOH systems was measured to be 5.3 Å and that describes the conformational changes of surface loops between these two systems (Fig. S17). The shape of the active site in hCEase_XOH system was totally disturbed especially the catalytic site core was distorted and is not appropriate for the binding of the substrate. This result was used as substantiation to the

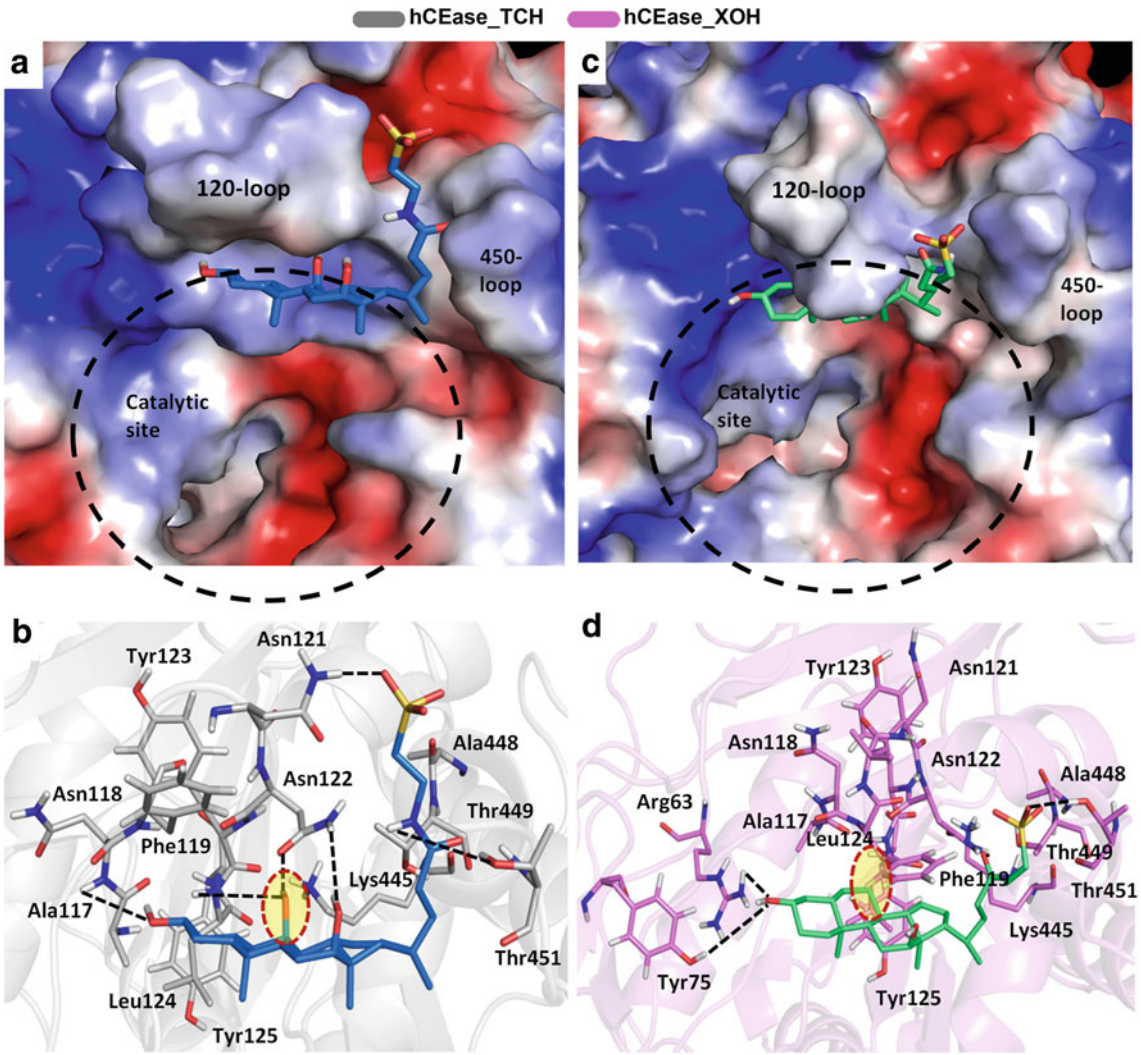

Fig. 8 Binding modes of TCH and TCH_XOH at the proximal site. The binding mode and H-bond interactions between protein and **a** TCH and **b** TCH_XOH are shown. TCH and TCH_XOH are shown in *blue* and *green color stick forms*. The missing 7 α-OH group region is highlighted in *red circles*. The H-bond interactions are shown in *black dashed lines*. The binding mode of TCH is stable and did not disturb the catalytic site. (Color figure online)

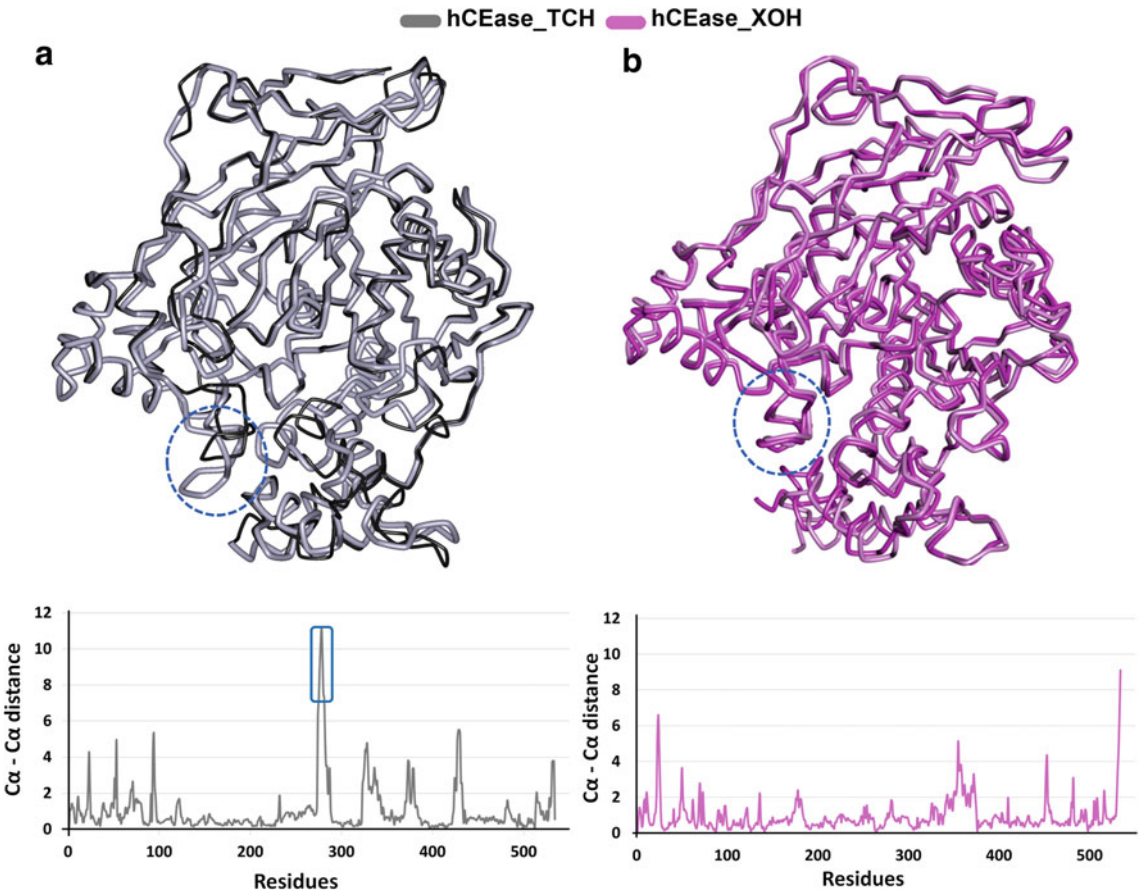

Fig. 9 Essential dynamics analysis. The maximum correlation motions were examined for hCEase_TCH and hCEase_XOH systems. The Cα–Cα distance plots between superimposed structures for each system are given below. The observed prominent movements are highlighted in *blue color circles*. (Color figure online)

importance of 7 α-OH group to form the interactions required for the activation of hCEase.

The ED analysis was carried out for hCEase_TCH and hCEase_XOH systems and Cα–Cα distance was measured to observe the predominant movement of the particular region of the protein which perhaps vital for its biological functions. The overlay of extreme structures, maximum and minimum projections of two protein trace, clearly explained that the predominant movement was observed in the 270-loop region when 7 α-OH group of TCH was present (Fig. 9a). Interestingly, movement of 270-loop was completely lost in the absence of 7 α-OH group (Fig. 9b). Thus, the absence of small functional groups like hydroxyl group can be able to demolish the possible activation of the protein. The maximum distance was observed around 270-loop residue in hCEase_TCH whereas this significant distance was totally lost in hCEase_XOH (Fig. 9). The results evidently showed that the specific interaction of 7 α-OH group of TCH plays a crucial role in the activation of the enzyme.

Conclusions

The hCEase has gained much attention as an interesting target in the treatment of major diseases like atherosclerosis and coronary heart disease due to its key role in the control of dietary cholesterols and the transport of free cholesterols to the enterocyte. A detailed structural knowledge of the activated form of hCEase is essential in designing potent drugs. To achieve this, MD simulation studies were carried out to understand the activation mechanism as well as to identify the molecular interactions and structural changes that are important for the bile salt activation of CEase were performed. Initially, the efficiency of different bile salts such as TCH, CHA, and GCH in the activation of hCEase was compared. From the binding mode, H-bond interaction, and distance analyses, it was concluded that the required movements of the surface loops are most favorable and the size of the active site was big enough when TCH is present. Hence, TCH was identified as the most favorable and efficient bile salt involved

in the activation of the hCEase. In the next study, after identifying the TCH as efficient bile salt, the involvement of both proximal and remote TCH in the activation mechanism of the hCEase was studied. From the results, it was observed that both bile salts are very important for the activation of hCEase. Especially the movement of the 120 and 270 loops, which is necessary for the binding of big substrate molecule, is much prominent when both bile salts are present. The synergistic effects of bile salts were observed when both proximal and remote bile salts are present as in the double-ligated system. As a third study, importance of 7 α-OH group of TCH in the activation of hCEase was carried out. From the results, it was revealed that 7 α-OH group is very important for the activation of hCEase. The molecular explanation is provided for the fact that a specific interaction through 7 α-OH group of bile salts is required for the hydrolysis of long chain substrate molecule. The results of our study have provided the deep structural insights, from various aspects, on the bile salt activation of hCEase and the key chemical characteristics of the bile salts influencing the activation. This detailed information will be helpful to avoid structural limitations when designing potent novel hCEase inhibitors. In addition, the activated structure can be used as a great starting point in structure-based drug design of efficient hypolipidemic agents.

Acknowledgments This research was supported by Basic Science Research Program (2012R1A1A4A01013657), Pioneer Research Center Program (2009-0081539), and Management of Climate Change Program (2010-0029084) through the National Research Foundation of Korea (NRF) funded by the Ministry of Education, Science and Technology (MEST) of Republic of Korea. And this work was also supported by the Next-Generation BioGreen 21 Program (PJ009486) from Rural Development Administration (RDA) of Republic of Korea.

References

1. Terzyan S, Wang C-S, Downs D, Hunter B, Zhang XC (2000) Crystal structure of the catalytic domain of human bile salt activated lipase. Protein Sci 9:1783–1790. doi:10.1110/ps.9.9.1783
2. Hui DY, Howles PN (2002) Carboxyl ester lipase. J Lipid Res 43:2017–2030. doi:10.1194/jlr.R200013-JLR200
3. Lin G, Liao W-C, Chiou S-Y (2000) Quantitative structure–activity relationships for the pre-steady-state inhibition of cholesterol esterase by 4-nitrophenyl-*n*-substituted carbamates. Bioorg Med Chem 8:2601–2607. doi:10.1016/s0968-0896(00)00196-6
4. Wang C-S, Hartsuck JA (1993) Bile salt-activated lipase. A multiple function lipolytic enzyme. Biochim Biophys Acta 1166:1–19. doi:10.1016/0005-2760(93)90277-g
5. Wang X, Wang C-S, Tang J, Dyda F, Zhang XC (1997) The crystal structure of bovine bile salt activated lipase: insights into the bile salt activation mechanism. Structure 5:1209–1218. doi:10.1016/s0969-2126(97)00271-2
6. Myers-Payne SC, Hui DY, Brockman HL, Schroeder F (1995) Cholesterol esterase: a cholesterol transfer protein. Biochemistry 34:3942–3947. doi:10.1021/bi00012a011
7. Howles PN, Carter CP, Hui DY (1996) Dietary free and esterified cholesterol absorption in cholesterol esterase (bile salt-stimulated lipase) gene-targeted mice. J Biol Chem 271:7196–7202. doi:10.1074/jbc.271.12.7196
8. Brodt-Eppley J, White P, Jenkins S, Hui DY (1995) Plasma cholesterol esterase level is a determinant for an atherogenic lipoprotein profile in normolipidemic human subjects. Biochim Biophys Acta 1272:69–72. doi:10.1016/0925-4439(95)00083-g
9. Bruneau N, Lombardo D, Bendayan M (1998) Participation of GRP94-related protein in secretion of pancreatic bile salt-dependent lipase and in its internalization by the intestinal epithelium. J Cell Sci 111:2665–2679
10. Heidrich J, Contos L, Hunsaker L, Deck L, Vander Jagt D (2004) Inhibition of pancreatic cholesterol esterase reduces cholesterol absorption in the hamster. BMC Pharmacol 4:5. doi:10.1186/1471-2210-4-5
11. Pietsch M, Gütschow M (2002) Alternate substrate inhibition of cholesterol esterase by thieno[2,3-*d*][1,3]oxazin-4-ones. J Biol Chem 277:24006–24013. doi:10.1074/jbc.M112252200
12. Lombardo D (2001) Bile salt-dependent lipase: its pathophysiological implications. Biochim Biophys Acta 1533:1–28. doi:10.1016/s1388-1981(01)00130-5
13. Deck LM, Baca ML, Salas SL, Hunsaker LA, Vander Jagt DL (1999) 3-Alkyl-6-chloro-2-pyrones: selective inhibitors of pancreatic cholesterol esterase. J Med Chem 42:4250–4256. doi:10.1021/jm990309x
14. Feaster SR, Lee K, Baker N, Hui DY, Quinn DM (1996) Molecular recognition by cholesterol esterase of active site ligands: structure–reactivity effects for inhibition by aryl carbamates and subsequent carbamylenzyme turnover. Biochemistry 35:16723–16734. doi:10.1021/bi961677v
15. John S, Thangapandian S, Lee KW (2012) Potential human cholesterol esterase inhibitor design: benefits from the molecular dynamics simulations and pharmacophore modeling studies. J Biomol Struct Dyn 29:921–936. doi:10.1080/07391102.2012.10507419
16. John S, Thangapandian S, Sakkiah S, Lee KW (2011) Discovery of potential pancreatic cholesterol esterase inhibitors using pharmacophore modelling, virtual screening, and optimization studies. J Enzyme Inhib Med Chem 26:535–545. doi:10.3109/14756366.2010.535795
17. Lin G, Shieh C-T, Ho H-C, Chouhwang J-Y, Lin W-Y, Lu C-P (1999) Structure–reactivity relationships for the inhibition mechanism at the second alkyl-chain-binding site of cholesterol esterase and lipase. Biochemistry 38:9971–9981. doi:10.1021/bi982775e
18. Cygler M, Schrag JD, Sussman JL, Harel M, Silman I, Gentry MK, Doctor BP (1993) Relationship between sequence conservation and three-dimensional structure in a large family of esterases, lipases, and related proteins. Protein Sci 2:366–382. doi:10.1002/pro.5560020309
19. Heynekamp JJ, Hunsaker LA, Vander Jagt TA, Royer RE, Deck LM, Vander Jagt DL (2008) Isocoumarin-based inhibitors of pancreatic cholesterol esterase. Bioorg Med Chem 16:5285–5294. doi:10.1016/j.bmc.2008.03.016
20. Rebaï O, Le Petit-Thevenin J, Bruneau N, Lombardo D, Vérine A (2005) In vitro angiogenic effects of pancreatic bile salt-dependent lipase. Arterioscler Thromb Vasc Biol 25:359–364. doi:10.1161/01.ATV.0000151618.49109.bd
21. Ollis DL, Cheah E, Cygler M, Dijkstra B, Frolow F, Franken SM, Harel M, Remington SJ, Silman I, Schrag J, Sussman JL, Verschueren KHG, Goldman A (1992) The α/β hydrolase fold. Protein Eng 5:197–211. doi:10.1093/protein/5.3.197
22. Quinn DM, Feaster SR (1998) In comprehensive biological catalysis. In: Sinnot M (ed) A mechanistic reference. Academic Press, San Diego, pp 455–482
23. Hernell O (1975) III. Physiological implications of the bile salt-stimulated lipase. Eur J Clin Invest 5:267–272. doi:10.1111/j.1365-2362.1975.tb02294.x

24. Fontbonne H, Brisson L, Vérine A, Puigserver A, Lombardo D, Ajandouz EH (2011) Human bile salt-dependent lipase efficiency on medium-chain acyl-containing substrates: control by sodium taurocholate. J Biochem 149:145–151. doi:10.1093/jb/mvq132
25. Hofmann AF, Borgstroem B (1964) The intraluminal phase of fat digestion in man: the lipid content of the micellar and oil phases of intestinal content obtained during fat digestion and absorption. J Clin Invest 43:247–257. doi:10.1172/jci104909
26. Bläckberg L, Hernell O (1993) Bile salt-stimulated lipase in human milk: evidence that bile salt induces lipid binding and activation via binding to different sites. FEBS Lett 323:207–210. doi:10.1016/0014-5793(93)81340-6
27. Berendsen HJC, van der Spoel D, van Drunen R (1995) GROMACS: a message-passing parallel molecular dynamics implementation. Comput Phys Commun 91:43–56. doi:10.1016/0010-4655(95)00042-e
28. Lindahl E, Hess B, van der Spoel D (2001) GROMACS 3.0: a package for molecular simulation and trajectory analysis. J Mol Model 7:306–317. doi:10.1007/s008940100045
29. Schüttelkopf AW, Van Aalten DMF (2004) PRODRG: a tool for high-throughput crystallography of protein–ligand complexes. Acta Crystallogr D Biol Crystallogr 60:1355–1363. doi:10.1107/s0907444904011679
30. Bussi G, Donadio D, Parrinello M (2007) Canonical sampling through velocity rescaling. J Chem Phys 126:014101–014107
31. Amadei A, Linssen ABM, Berendsen HJC (1993) Essential dynamics of proteins. Proteins 17:412–425. doi:10.1002/prot.340170408
32. García AE (1992) Large-amplitude nonlinear motions in proteins. Phys Rev Lett 68:2696–2699
33. Van Aalten DMF, Findlay JBC, Amadei A, Berendsen HJC (1995) Essential dynamics of the cellular retinol-binding protein evidence for ligand-induced conformational changes. Protein Eng 8:1129–1135. doi:10.1093/protein/8.11.1129
34. Chau PL, van Aalten DMF, Bywater RP, Findlay JBC (1999) Functional concerted motions in the bovine serum retinol-binding protein. J Comput Aided Mol Des 13:11–20. doi:10.1023/a:1008099903676
35. de Groot BL, van Aalten DM, Amadei A, Berendsen HJ (1996) The consistency of large concerted motions in proteins in molecular dynamics simulations. Biophys J 71:1707–1713
36. Horstink LM, Abseher R, Nilges M, Hilbers CW (1999) Functionally important correlated motions in the single-stranded DNA-binding protein encoded by filamentous phage Pf3. J Mol Biol 287:569–577. doi:10.1006/jmbi.1999.2629
37. Peters GH, Bywater RP (1999) Computational analysis of chain flexibility and fluctuations in *Rhizomucor miehei* lipase. Protein Eng 12:747–754. doi:10.1093/protein/12.9.747
38. Peters GH, Frimurer TM, Andersen JN, Olsen OH (1999) Molecular dynamics simulations of protein-tyrosine phosphatase 1B. I. Ligand-induced changes in the protein motions. Biophys J 77:505–515
39. Peters GH, van Aalten DM, Edholm O, Toxvaerd S, Bywater R (1996) Dynamics of proteins in different solvent systems: analysis of essential motion in lipases. Biophys J 71:2245–2255
40. Stella L, Di Iorio EE, Nicotra M, Ricci G (1999) Molecular dynamics simulations of human glutathione transferase P1-1: conformational fluctuations of the apo-structure. Proteins 37:10–19. doi:10.1002/(sici)1097-0134(19991001)37:1<10::aid-prot2>3.0.co;2-0
41. van Aalten DM, Amadei A, Bywater R, Findlay JB, Berendsen HJ, Sander C, Stouten PF (1996) A comparison of structural and dynamic properties of different simulation methods applied to SH3. Biophys J 70:684–692
42. van Aalten DM, Hoff WD, Findlay JB, Crielaard W, Hellingwerf KJ (1998) Concerted motions in the photoactive yellow protein. Protein Eng 11:873–879. doi:10.1093/protein/11.10.873
43. van Aalten DMF, Amadei A, Linssen ABM, Eijsink VGH, Vriend G, Berendsen HJC (1995) The essential dynamics of thermolysin: confirmation of the hinge-bending motion and comparison of simulations in vacuum and water. Proteins 22:45–54. doi:10.1002/prot.340220107
44. Arcangeli C, Bizzarri AR, Cannistraro S (2001) Concerted motions in copper plastocyanin and azurin: an essential dynamics study. Biophys Chem 90:45–56. doi:10.1016/s0301-4622(01)00128-4
45. Lee Y, Bang WY, Kim S, Lazar P, Kim CW, Bahk JD, Lee KW (2010) Molecular modeling study for interaction between *Bacillus subtilis* Obg and nucleotides. PLoS ONE 5:e12597. doi:10.1371/journal.pone.0012597
46. Wallace AC, Laskowski RA, Thornton JM (1995) LIGPLOT: a program to generate schematic diagrams of protein–ligand interactions. Protein Eng 8:127–134. doi:10.1093/protein/8.2.127
47. Stierand K, Maaß PC, Rarey M (2006) Molecular complexes at a glance: automated generation of two-dimensional complex diagrams. Bioinformatics 22:1710–1716. doi:10.1093/bioinformatics/btl150
48. Ghosh D, Wawrzak Z, Pletnev VZ, Li N, Kaiser R, Pangborn W, Jörnvall H, Erman M, Duax WL (1995) Structure of uncomplexed and linoleate-bound *Candida cylindracea* cholesterol esterase. Structure 3:279–288. doi:10.1016/s0969-2126(01)00158-7
49. Grochulski P, Bouthillier F, Kazlauskas RJ, Serreqi AN, Schrag JD, Ziomek E, Cygler M (1994) Analogs of reaction intermediates identify a unique substrate binding site in *Candida rugosa* lipase. Biochemistry 33:3494–3500. doi:10.1021/bi00178a005
50. Kim KK, Song HK, Shin DH, Hwang KY, Suh SW (1997) The crystal structure of a triacylglycerol lipase from *Pseudomonas cepacia* reveals a highly open conformation in the absence of a bound inhibitor. Structure 5:173–185. doi:10.1016/s0969-2126(97)00177-9
51. Schrag JD, Li Y, Cygler M, Lang D, Burgdorf T, Hecht H-J, Schmid R, Schomburg D, Rydel TJ, Oliver JD, Strickland LC, Dunaway CM, Larson SB, Day J, McPherson A (1997) The open conformation of a Pseudomonas lipase. Structure 5:187–202. doi:10.1016/s0969-2126(97)00178-0